Dirichlet energy of Delaunay meshes and intrinsic Delaunay triangulations

Zipeng Ye [a], Ran Yi [a], Wenyong Gong [b,*], Ying He [c], Yong-Jin Liu [a]

[a] *BNRist, MOE-Key Laboratory of Pervasive Computing, The Department of Computer Science and Technology, Tsinghua University, Beijing, China*
[b] *Department of Mathematics, Jinan University, Guangzhou, China*
[c] *School of Computer Engineering, Nanyang Technological University, Singapore*

ARTICLE INFO

ABSTRACT

The Dirichlet energy of a smooth function measures how variable the function is. Due to its deep connection to the Laplace–Beltrami operator, Dirichlet energy plays an important role in digital geometry processing. Given a 2-manifold triangle mesh M with vertex set V, the generalized Rippa's theorem shows that the Dirichlet energy among all possible triangulations of V arrives at its minimum on the intrinsic Delaunay triangulation (IDT) of V. Recently, Delaunay meshes (DM) – a special type of triangle mesh whose IDT is the mesh itself – were proposed, which can be constructed by splitting mesh edges and refining the triangulation to ensure the Delaunay condition. This paper focuses on Dirichlet energy for functions defined on DMs. Given an arbitrary function f defined on the original mesh vertices V, we present a scheme to assign function values to the DM vertices $V_{new} \supset V$ by interpolating f. We prove that the Dirichlet energy on DM is no more than that on the IDT. Furthermore, among all possible functions defined on V_{new} by interpolating f, our scheme attains the global minimum of Dirichlet energy on a given DM.

© 2020 Elsevier Ltd. All rights reserved.

1. Introduction

In mathematics, the Dirichlet energy of a smooth function measures how variable the function is. Since it is intimately linked with Laplace's equation, the Dirichlet energy has been widely used in many engineering fields, such as numerical solutions to PDE and data clustering (e.g., [1]). In computer graphics and computational geometry, the Dirichlet energy defined on polyhedral surfaces is of particular interest, and has been widely studied in the past three decades (e.g., [2–4]).

Delaunay triangulation is closely related to the Dirichlet energy. Rippa's theorem [2] reveals that in Euclidean spaces, the Dirichlet energy attains its minimum on Delaunay triangulations. A Delaunay triangulation for a given set P of 2D points is a triangulation DT on P such that no point in P is inside the circumcircle of any triangle in DT. Delaunay triangulation has many properties favorable to digital geometry processing (e.g., [5–8]). For example, it maximizes the minimum angle of all the angles of the triangles in the triangulation, hereby tending to avoid sliver triangles.

Although Delaunay triangulation in Euclidean spaces is well understood, only in recent years Delaunay triangulation on curved manifolds has received attention. The manifold counterpart, called *intrinsic Delaunay triangulation (IDT)* [9], is a triangulation defined

on a polyhedral surface and with geodesic edges (see Fig. 1(b)). An IDT has exactly the same geometry of the polyhedral surface, since no new vertices are required to form the triangulation. However, an IDT may contain degenerate faces with only two vertices or edges. Bobenko and Springborn [4] showed that Rippa's theorem also holds for polyhedral surfaces: given a 2-manifold polygonal mesh M with vertex set V, the minimum of the Dirichlet energy among all possible geodesic triangulations of V on M is attained on the intrinsic Delaunay triangulation, where V is the set of mesh vertices in M. Since the sum of the angles opposite an internal edge does not exceed π, the IDT-induced cotangent Laplace operator [10] is guaranteed to have non-negative weights, which is highly desirable in digital geometry processing.

Delaunay mesh (DM) is a special 2-manifold triangle mesh whose IDT is the mesh itself [11,12]. Thanks to its many favorable features [11–14], DM is an effective mesh representation scheme that can improve the accuracy and the robustness of PDE-based numerical computation, such as geodesic computation [15] and harmonic parameterization [3]. Liu et al. [12] developed an algorithm to convert an arbitrary manifold triangle mesh M with m vertices into a DM with $O(Km)$ vertices in $O(mK\log K)$ time, where K is a model-dependent constant. Their algorithm adds auxiliary points to the edges of M and locally refines incident faces to ensure the Delaunay condition. They showed that the resulting DM has the same geometry of the input mesh M (Fig. 1(c)), thus the Hausdorff distance between M and DM is zero, which in turns

(a) Original mesh   (b) IDT   (c) DM
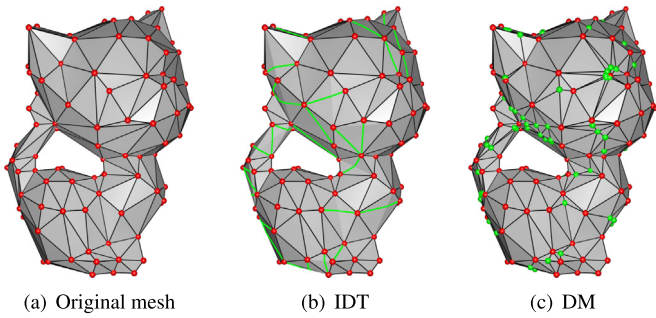
Fig. 1. Both intrinsic Delaunay triangulation and Delaunay mesh have the same geometry of the input triangle mesh M. IDT shares the same vertex set of M (red), but its edges are geodesics (green polylines) that may cross several triangular faces. DM contains auxiliary vertices (green dots) and its edges are line segments. (For interpretation of the references to color in this figure legend, the reader is referred to the web version of this article.)

implies the Hausdorff distance between IDT and DM is also zero. It is worth noting that for a given 2-manifold mesh M, there are infinitely many Delaunay meshes with the same geometry of M.

The existing algorithms mainly focus on constructing IDTs and DMs [11–13,16]. In this paper, we study the relation of Dirichlet energies on DM and IDT. Although both DM and IDT have the same geometry with the original mesh M, DM has more vertices than IDT. Given any function f defined on the vertices of M, we propose a scheme to assign function values on the newly added vertices in DM by interpolating f. Then we present a constructive proof, showing that the resulting Dirichlet energy on any DMs is no more than the Dirichlet energy on the IDT of M. We also show that among all possible interpolating functions defined on the vertices of DM, our proposed scheme attains the global minimum of Dirichlet energy. Our scheme does not need to compute IDT explicitly, which is usually difficult to represent since its edges are geodesics that may cross multiple triangles.

Designing a scheme for interpolating function values on mesh vertices is desired in many geometric processing applications. In some application scenarios, computing the features of a part of vertices in a mesh is easy, but computing the features of all points is hard. However a proper interpolation technique can offer an available resolution to this issue. For example, it is possible to fast query geodesic distance on triangle meshes with the help of interpolation techniques [17].

Our contributions are twofold. First, we propose a holistic COT harmonic interpolation scheme for newly added vertices in DM, and prove that the interpolation attains the unique global minimum of the Dirichlet energy on DM. Second, for a given 2-manifold mesh, the relation of Dirichlet energy between corresponding IDT and DM is compared according to our interpolation scheme, which is not reported in the existing literature.

The rest of this paper is organized as follows. Section 2 reviews the related work and present background knowledge. Section 3 presents the main theoretical results, followed by experiments and applications in Section 4. Section 5 concludes the paper.

2. Related work & preliminaries

In this section, we briefly review the most related work of Dirichlet energy and Delaunay triangulations. We refer readers to [5,6] for a comprehensive review.

Denote by $M = (V, E, F)$ the manifold triangle mesh and V, E and F its sets of vertices, edges and faces. Each edge carries an arbitrary but fixed orientation, while vertices and triangles always have counterclockwise orientation by convention. Index order indicates direction, in the sense that edge e_{ij} is directed

from vertex v_i to v_j. For a triangular face $f_{ijk} = (v_i, v_j, v_k)$, we denote the angle between e_{jk} and e_{ji} by α_{ik}. If multiple triangles are involved and ambiguity occurs, we use the full indices to denote angle, e.g., $\alpha_{ijk} = \angle v_i v_j v_k$.

2.1. Dirichlet Energy

Let $\Gamma = \{T_i\}$ be all geodesic triangulations on a 2-manifold mesh M, in which each T_i has the same set of vertices with M. Let $V = \{v_1, v_2, \ldots, v_m\}$, E_T and F_T be the sets of vertices, edges and triangular faces of a geodesic triangulation $T \in \Gamma$ on the domain M, respectively. Note that $M \in \Gamma$ since it is a special triangulation in Γ. Let $f : V \to \mathbb{R}$ be a scalar function defined on vertices V. For each $T \in \Gamma$, let $f|_T : T \to \mathbb{R}$ be a piecewise linear function interpolating f on T, $f|_T(v_i) = f(v_i)$, $\forall v_i \in V$, i.e., $f|_T$ is linear on the faces of T and its gradient $\nabla f|_T$ is a constant vector on each face.

The Dirichlet energy of $f|_T$ on T is

$$\mathcal{E}(f|_T) = \frac{1}{2} \int_T \|\nabla f_T\|^2 dA \tag{1}$$

Using the finite element method [10,18], the Dirichlet energy is discretized as

$$\mathcal{E}(f|_T) = \frac{1}{4} \sum_{f_{ijk} \in F_T} [\cot \alpha_{ij}(f_i - f_j)^2 + \\ \cot \alpha_{jk}(f_j - f_k)^2 + \cot \alpha_{ki}(f_k - f_i)^2] \tag{2}$$

where $f_l = f(v_l)$. Rearranging the terms in Eq. (2) leads to a sum over the edges of T

$$\mathcal{E}(f|_T) = \frac{1}{2} \sum_{e_{ij} \in E_T} \omega_{ij}(f_i - f_j)^2, \tag{3}$$

where $\omega_{ij} = \frac{1}{2}(\cot \alpha_{ij} + \cot \beta_{ij})$, $\alpha_{ij} = \angle v_i v_p v_j$ and $\beta_{ij} = \angle v_i v_q v_j$ are opposite angles in two faces adjacent to the edge e_{ij}.

The Dirichlet energy is closely related to Laplace's equation, since the solutions of Laplace's equation are harmonic functions, which are smooth functions minimizing the Dirichlet energy [19]. The Laplace operator, given by the divergence of the gradient of a function on Euclidean space, can be generalized to operate on functions defined on Riemannian manifolds. This generalized operator is often called Laplace–Beltrami operator (LBO). Discrete LBOs on polygonal surfaces have attracted considerable research and found a wide range of applications in computer graphics and computer vision [4,10,18,20–24]. Xu and his colleagues [25,26] presented deep investigation on the Dirichlet energy defined on triangular/quadrilateral meshes and the convergence of different discrete LBO schemes.

2.2. Intrinsic delaunay triangulation

Bobenko and Springborn [4] defined the IDT associated to M as follows:

- the IDT's vertex set is the same as that of M,
- every IDT edge is a geodesic path in M,
- for each interior edge, the local Delaunay criterion is satisfied, i.e., the sum of the opposite angles in the adjacent triangles is no more than π.

Rivin [9] conjectured that the IDT can be constructed by edge flipping without rigorous proofs. Bobenko and Springborn [4] proved that by iteratively flipping the non-Delaunay geodesic edges to be locally Delaunay, the edge flipping algorithm terminates in a finite number of steps, implying that the intrinsic Delaunay triangulation exists. They also proved the uniqueness
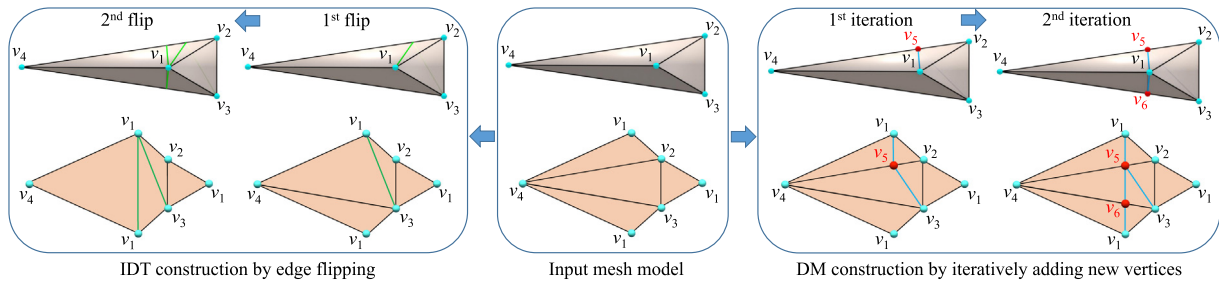
Fig. 2. IDT and DM construction on a tetrahedron. The top row shows the tetrahedron rendered semitransparent and the bottom row shows the flattened 2D triangulation. The original tetrahedron is very long and narrow. For better illustration, a nonuniform scaling is used. The vertex coordinates are $v_1 = (0.005, 0.0, 0.130)$, $v_2 = (1.732, 1.0, 0.0)$, $v_3 = (1.732, -1.0, 0.0)$ and $v_4 = (-100.0, 0.0, 0.0)$. The resulting IDT has a self-loop edge at v_1 and then each of its two adjacent faces has only two vertices. DM is constructed by iteratively adding new vertices, i.e., $v_5 = (0.0, 0.983, 0.0)$ and $v_6 = (0.0, -0.983, 0.0)$, into the tetrahedron with face subdivision.

of Delaunay tessellation[1] and the IDT can be obtained by triangulating the non-triangular faces. Afterwards, Fisher et al. [27] presented a practical edge-flipping algorithm to compute the IDT from an arbitrary triangle mesh. The edge-flipping algorithm [4,27] does not have known time complexity and may also produce geodesic triangulations containing faces with only two vertices or only two edges, or edges adjacent to the same face on both sides. See Fig. 2 left for an example. Liu et al. [16] developed an algorithm for constructing *proper*[2] IDTs from the dual of geodesic Voronoi diagram. Their algorithm runs in $O(m^2 + tm \log m)$ time, where t is the number of obtuse angles in the mesh. The widely used cotangent LBO always has non-negative weights on IDTs and thus numerical stability can be achieved in many computer graphics applications [27]. Recently Sharp et al. [28] customized an efficient data structure that stores the direction and distance to neighboring vertices. Then IDTs can be viewed as ordinary meshes, and common geometric operations and algorithms can be easily implemented.

Bobenko and Springborn [4] generalized Rippa's theorem [2], showing that among all geodesic triangulations in Γ, the minimum of the Dirichlet energy defined in Eq. (1) is attained on IDT I_M,

$$\min_{T \in \Gamma} \frac{1}{2} \int_T \|\nabla f|_T\|^2 dA = \frac{1}{2} \int_{I_M} \|\nabla f|_{I_M}\|^2 dA. \qquad (4)$$

2.3. Delaunay meshes

As a special type of IDT, DMs are triangle meshes where the local Delaunay condition holds everywhere. Dyer et al. [11] developed an algorithm to convert an arbitrary triangle mesh M into a DM by recursively splitting non-Delaunay edges and refine the local triangulations. Both M and DM have the same geometry. However, their algorithm can only prove the convergence without time and space complexity. In practice, since their local refinement scheme is purely combinatorial and does not consider the local geometry, their algorithm often adds too many redundant splitting points into the mesh.

Recently, Liu et al. [12] proposed a geometry-aware algorithm for constructing DM. An edge e in M is *locally Delaunay* (LD) if the sum of the two angles facing e is no more than π; otherwise it is *non-locally Delaunay* (NLD). An NLD edge is called planar if its two incident faces are coplanar, and non-planar otherwise. Liu et al. propose a Delaunay sampling criterion, based on which a set of candidate points S are sampled on edges in M. Then their algorithm flips planar NLD edges and iteratively processes non-planar NLD edges e by adding selected auxiliary points from S

based on the local geometry around e (Fig. 2 right). Splitting edges and faces at auxiliary points will introduce more edges and faces into M, which may also turn some existing LD edges into NLD. Liu et al. [12] proved that the iterative process is guaranteed to terminate and their algorithm runs in $O(K'n)$ time, where K' is a constant depending on model's geometry.

3. Main theoretical result

Throughout this paper, given an arbitrary 2-manifold triangle mesh $M = (V, E, F)$, we denote the IDT and any DM of M as I_M and D_M, respectively. The sets of vertices, edges and faces of I_M and D_M are denoted as $(V_I = V, E_I, F_I)$ and (V_D, E_D, F_D), respectively.

The generalized Rippa's theorem [4] shows that among all possible geodesic triangulations of V on the manifold domain M, the Dirichlet energy arrives at its minimum when the triangulation is intrinsically Delaunay. On the other hand, the recently proposed DM is a special IDT by adding more vertices into IDT of M. In this paper, we study the relation of Dirichlet energies on D_M and I_M that has the same geometry of M.

We assume that all Delaunay meshes D_M studied in this paper are in general position, i.e., for any interior edge $e_{ij} \in E_D$, the sum of its opposite angles α_{ij} and β_{ij} in two faces adjacent to e is strictly less than π; in other words, when folding two faces sharing e into a common plane, no circle passes through their four vertices. This general assumption is easy to guarantee during the DM construction process: for any new inserted vertex, if degeneracy occurs, a tiny perturbation is sufficient to remove it. In fact, the assumption implies the global unique minimizer of Laplace's equations with given boundary conditions.

3.1. Minimization of Dirichlet energy on D_M

Different from IDT, DM has more vertices and the vertex set V_D of D_M can be separated into two mutually exclusive subsets: the vertex set V of M and the new vertex set $V_D \setminus V$. Given any function $f : V \to \mathbb{R}$, to compute Dirichlet energy on D_M, the function values of vertices in $V_D \setminus V$ need to be determined. Since the DM construction algorithm [12] adds new vertices only at the edges $e \in E$ of M, intuitively, barycentric interpolation or other special schemes (e.g., incremental cotan interpolation illustrated below in Example 3.3) during DM construction can be used. However, both barycentric interpolation and incremental cotan interpolation may lead to larger Dirichlet energy values than that of IDT. The main reason is that both interpolation methods cannot achieve globally optimal result. Below we use M, I_M and D_M in Fig. 2 as illustrative examples.

---

[1] Faces in Delaunay tessellation are general but not always triangular.

[2] An IDT is proper if it is a realization of a simplicial complex. All Delaunay triangulations in $\mathbb{R}^2$ are proper.

Example 3.1. Let $f|_M \colon F_M \to \mathbb{R}$ and $f|_{I_M} \colon F_I \to \mathbb{R}$ be the piecewise linear functions with $f(v_1) = 1, f(v_2) = 2, f(v_3) = 2$ and $f(v_4) = 2$ on the face sets $F_M = (\triangle v_1 v_3 v_2, \triangle v_1 v_4 v_3, \triangle v_1 v_2 v_4, \triangle v_2 v_3 v_4)$ of the original tetrahedron mesh M and $F_I = (\triangle v_1 v_3 v_2, \triangle \widetilde{v_1 v_3 v_2},$ $\triangle \widetilde{v_1 v_1 v_3}, \triangle \widetilde{v_1 v_1 v_4})$ of the IDT I_M of M, respectively, where $\triangle \widetilde{v_1 v_3 v_2}, \triangle \widetilde{v_1 v_1 v_3}$ and $\triangle \widetilde{v_1 v_1 v_4}$ are triangles with curved geodesic edges. The Dirichlet energies on M and I_M are $\mathcal{E}(f|_M) = 201.232$ and $\mathcal{E}(f|_{I_M}) = 4.659$.

Example 3.2. Let $f(v_1) = 1, f(v_2) = 2, f(v_3) = 2$ and $f(v_4) = 2$, the same as in Example 3.1. The DM D_M adds two new vertices v_5 and v_6 into the original tetrahedron mesh M. Given that v_5 lies on the edge (v_2, v_4) and v_6 lies on the edge (v_3, v_4), using barycentric interpolation, we have $f(v_5) = 2$ and $f(v_6) = 2$. Then the Dirichlet energy on D_M is $\mathcal{E}(f|_{D_M}) = 201.232$, which is the same as $\mathcal{E}(f|_M)$ and larger than $\mathcal{E}(f|_{I_M})$, where $f|_{D_M} \colon F_D \to \mathbb{R}$ is the piecewise linear function on the face set F_D of D_M, interpolating the function values $f(v_i), i = 1, 2, \ldots, 6$.

Example 3.3. Let $f(v_1) = 1, f(v_2) = 2, f(v_3) = 2, f(v_4) = 2$, the same as in Example 3.1. In the DM construction process, first v_5 is added on the edge (v_2, v_4), which is adjacent to faces $\triangle v_1 v_2 v_4$ and $\triangle v_2 v_3 v_4$. Using cotan interpolation, we minimize the following quantity with variable $f(v_5)$:

$$\frac{1}{4}[(\cot \alpha_{145} + \cot \alpha_{125})(f(v_1) - f(v_5))^2 + \\ (\cot \alpha_{215} + \cot \alpha_{235})(f(v_2) - f(v_5))^2 + \\ (\cot \alpha_{325} + \cot \alpha_{345})(f(v_3) - f(v_5))^2 + \\ (\cot \alpha_{415} + \cot \alpha_{435})(f(v_4) - f(v_5))^2] \tag{5}$$

and we have $f(v_5) = 1.35$. Second, v_6 is added on the edge (v_3, v_4), which is adjacent to faces $\triangle v_3 v_4 v_5$ and $\triangle v_1 v_3 v_4$. Using cotan interpolation again, we minimize the following quantity with variable $f(v_6)$:

$$\frac{1}{4}[(\cot \alpha_{136} + \cot \alpha_{146})(f(v_1) - f(v_6))^2 + \\ (\cot \alpha_{316} + \cot \alpha_{356})(f(v_3) - f(v_6))^2 + \\ (\cot \alpha_{416} + \cot \alpha_{456})(f(v_4) - f(v_6))^2 + \\ (\cot \alpha_{536} + \cot \alpha_{546})(f(v_5) - f(v_6))^2] \tag{6}$$

and we have $f(v_6) = 1.13$. Then the Dirichlet energy on D_M is $\mathcal{E}(f|_{D_M}) = 19.672$, which is larger than $\mathcal{E}(f|_{I_M})$, where $f|_{D_M} \colon F_D \to \mathbb{R}$ is the piecewise linear function on the face set F_D of D_M, interpolating the function values $f(v_i), i = 1, 2, \ldots, 6$.

There exist infinitely possible interpolating schemes to extend an arbitrary scalar function f defined on V to vertices in $V_D \setminus V$, including the barycentric interpolation and incremental cotan interpolation in Examples 3.2 and 3.3. Below we propose a novel holistic COT harmonic interpolation, with three distinct merits: (1) we prove that it achieves the minimum of Dirichlet energy on D_M among all possible interpolating schemes, (2) we prove that it has lower Dirichlet energy than that of IDT, and (3) it does not depend on the IDT and thus is easy to compute.

Proposition 3.1 (*Holistic COT Harmonic Interpolation*). *Given a 2-manifold mesh M, a scalar function $f \colon V \to \mathbb{R}$ defined on vertices V of M and a Delaunay mesh D_M of M, the following linear system of equations has a unique solution to unknown scalars $f_{m+1}, f_{m+2}, \ldots, f_n$ that are function values at vertices in $V_D \setminus V$ of D_M:*

$$\sum_{v_j \in nbhd(v_i)} (\cot \alpha_{ij} + \cot \beta_{ij})(f_i - f_j) = 0, \\ i = m + 1, m + 2, \ldots, n \tag{7}$$

where m and n are numbers of vertices in V and V_D respectively, $nbhd(v_i)$ of $v_i \in V_D$ contains those vertices sharing an edge with v_i in D_M and $f_1, f_2 \cdots, f_m$ are known function values at vertices V specified by $f \colon V \to \mathbb{R}$.

Proof. We rearrange the terms in the linear system (7) by putting unknowns on the left and constants on the right:

$$\sum_{v_j \in nbhd(v_i)} (\cot \alpha_{ij} + \cot \beta_{ij}) f_i - \\ \sum_{v_j \in nbhd(v_i), j > m} (\cot \alpha_{ij} + \cot \beta_{ij}) f_j \\ = \sum_{v_j \in nbhd(v_i), j \le m} (\cot \alpha_{ij} + \cot \beta_{ij}) f_j \\ i = m + 1, m + 2, \ldots, n \tag{8}$$

which can be written in a matrix form as

$$\mathbf{A}\mathbf{x} = \mathbf{b}, \tag{9}$$

where $\mathbf{A}$ is an $(n - m) \times (n - m)$ matrix, $\mathbf{x}$ is a $(n - m) \times 1$ column vector $(f_{m+1} \ f_{m+2} \ \cdots \ f_n)^T$ which contains all unknowns and $\mathbf{b}$ is a constant $(n - m) \times 1$ column vector.

To prove that the system in Eq. (9) has a unique solution, we need to show that the matrix $\mathbf{A}$ is invertible. In the proof of Theorem 3.1 presented below, we prove that $\mathbf{A}$ is positive definite and then is invertible. $\square$

Theorem 3.1. *Given a 2-manifold mesh M, a Delaunay mesh D_M of M and a scalar function $f \colon V \to \mathbb{R}$ defined on vertices V of M, in all possible scalar function $f_D \colon V_D \to \mathbb{R}$ defined on vertices V_D of D_M that satisfies $f_D(v) = f(v), \forall v \in V$, the function f_D^* attains the global minimum of Dirichlet energy of $f_D|_{D_M}$ on $D_M = (V_D, E_D, F_D)$:*

$$\mathcal{E}(f_D^*|_{D_M}) = \frac{1}{4} \sum_{e_{i,j} \in E_D} (\cot \alpha_{ij} + \cot \beta_{ij})(f_i - f_j)^2 \tag{10}$$

where $f_D^*|_{D_M} \colon F_D \to \mathbb{R}$ is a piecewise linear function on F_D with $f_D^*|_{D_M}(v_i) = f_D^*(v_i), \forall v_i \in V_D$, if and only if f_D^* is given by holistic COT harmonic interpolation in Proposition 3.1 .

Proof. Note that $\nabla \mathcal{E}(f_D|_{D_M}) = 0$ with respect to the unknowns $\mathbf{x} = (f_{m+1} \ f_{m+2} \ \cdots \ f_n)^T$ (whose elements are function values at $V_D \setminus V$ of D_M) is exactly the linear system of Eqs. (7). Below we show that the quadratic function $\mathcal{E}(f_D|_{D_M})$ is convex; therefore, $\nabla \mathcal{E}(f_D^*|_{D_M}) = 0$ implies that $\mathcal{E}(f_D^*|_{D_M})$ is a global minimizer.

A twice continuously differentiable function is strictly convex if and only if its Hessian matrix is positive definite. Eq. (10) can be rewritten in a matrix form as $\mathbf{x}^T \mathbf{A} \mathbf{x} + \mathbf{b}\mathbf{x} + c$, where the symmetric matrix $\mathbf{A}$ is specified in Eq. (9), $\mathbf{b}$ is a $1 \times (n - m)$ constant vector and c is a constant. Then the Hessian matrix of $\mathcal{E}$ is $\mathbf{A}$. Below we show that $\mathbf{A}$ is positive definite.

First, $\forall \mathbf{x} = (f_{m+1} \ f_{m+2} \ \cdots \ f_n)^T$, we have

$$\mathbf{x}^T \mathbf{A} \mathbf{x} = \frac{1}{4} \sum_{e_{i,j} \in E_D, i > m, j > m} (\cot \alpha_{ij} + \cot \beta_{ij})(f_i - f_j)^2 \\ + \frac{1}{4} \sum_{e_{i,j} \in E_D, i > m \ge j} (\cot \alpha_{ij} + \cot \beta_{ij}) f_i^2 \tag{11}$$

Given that due to the local Delaunay condition, $\cot \alpha_{ij} + \cot \beta_{ij} > 0, \forall i, j$, we have $\mathbf{x}^T \mathbf{A} \mathbf{x} \ge 0$. Next, we show that $\mathbf{x}^T \mathbf{A} \mathbf{x} = 0$ if and only if $\mathbf{x} = 0$.

By Eq. (11), $\mathbf{x}^T \mathbf{A} \mathbf{x} = 0$ implies two conditions:

$$\sum_{e_{i,j} \in E_D, i > m, j > m} (\cot \alpha_{ij} + \cot \beta_{ij})(f_i - f_j)^2 = 0 \tag{12}$$

and

$$\sum_{e_{i,j} \in E_D, i > m \ge j} (\cot \alpha_{ij} + \cot \beta_{ij}) f_i^2 = 0 \tag{13}$$

If $\mathbf{A}$ is irreducible, all vertices in $V_D \setminus V$ are connected in D_M. The condition in Eq. (12) implies that all the values in $\mathbf{x}$ are equal. The condition in Eq. (13) implies that at least one value in $\mathbf{x}$ is zero. Therefore, both conditions imply $\mathbf{x} = 0$. If $\mathbf{A}$ is reducible, $\mathbf{A}$ can be rearranged into block upper-triangular form by simultaneous row/column permutations. Now we examine each block submatrix, denoted as $\mathbf{A}_i$, which is irreducible. Since $\mathbf{A}_i$ is irreducible, by replacing non-zero entries in $\mathbf{A}_i$ by one and

viewing the matrix as the adjacency matrix of a graph g_i, we have that (1) g_i is strongly connected and (2) in each g_i at least one vertex has neighbors in V. Then the condition in Eq. (12) implies that all the function values at vertices in g_i are equal, and the condition in Eq. (13) implies that at least one vertex's value in g_i is zero. Therefore, both conditions imply that all the function values at vertices in each g_i are zero and then $\mathbf{x} = 0$. That completes the proof. □

There exist simple methods that can prove the positive definiteness of A in previous Proposition and Theorem. E.g., according to the rank (equal to n-1) of the Laplacian matrix and given boundary conditions, we can result in the positive definiteness, but here we adopt a complete proof that can be self-contained. Note that the proofs stated above are valid for closed meshes. In fact, the Proposition 3.1 is also true for 2-manifold meshes with boundaries. The Dirichlet energy in (10) is convex on any 2-manifold meshes, then the null space of Laplacian operator is a constant function, and the Laplacian matrix can be non-singular. Since the matrix in (7) is a sub-matrix of the Laplacian matrix, then it is also non-singular, therefore a unique solution can also be guaranteed.

3.2. Relation of Dirichlet energies on D_M and I_M

Both DM D_M and IDT I_M satisfy local Delaunay condition on every (geodesic) edge, and they have the same geometry of the original mesh M. In this section, we show that using the holistic COT harmonic interpolation in Proposition 3.1, the Dirichlet Energy on D_M is no greater than that on I_M.

To establish such a relation, our strategy is to propose an interpolation scheme that starts from I_M, iteratively adds new vertices in $V_D \setminus V$ and updates the mesh connectivity, and finally reaches D_M.

Given any $f : V \to \mathbb{R}$, the Dirichlet Energy on $I_M = (V_I = V, E_I, F_I)$ is

$$\mathcal{E}(f|_{I_M}) = \frac{1}{4} \sum_{e=(v_i,v_j)\in E_I} (\cot \alpha_{ij} + \cot \beta_{ij})(f_i - f_j)^2 \quad (14)$$

where $f|_{I_M}: F_I \to \mathbb{R}$ is a piecewise linear function on F_I with $f|_{I_M}(v_i) = f(v_i), \forall v_i \in V_I$.

We put the vertices in $V_D \setminus V_I$ into a sorted[3] list $L = \{v_{m+1}, v_{m+2}, \dots, v_n\}$. Let $M_m = I_M$. Starting from $i = m + 1$, we iteratively assign the function value at v_i and subdivide the mesh using the following steps:

- Step 1. Find the geodesic edge $e_{p,q} \in E_{M_{i-1}}$ or the geodesic face $f_{abc} \in F_{M_{i-1}}$ whose interior contains v_i.
- Step 2. Assign the value $f(v_i)$ using the barycentric interpolation between $f(v_p)$ and $f(v_q)$, or among $f(v_a), f(v_b)$ and $f(v_c)$.
- Step 3. Add v_i and locally subdivide M_{i-1} into a 2-manifold mesh $M'_i = (V_{M'_i}, E_{M'_i}, F_{M'_i})$, $v_i \in V_{M'_i}$;
- Step 4. Apply the edge flipping algorithm [4,27] to M'_i and generate an IDT of M'_i; denote the resulting IDT as $M_i = (V_{M_i} = V_{M'_i}, E_{M_i}, F_{M_i})$.
- Step 5. If $i < n$, then $i \leftarrow i + 1$ and go to Step 1; otherwise stop.

In above iterative process, let $f_{M'_i}|_{M'_i}: F_{M'_i} \to \mathbb{R}$ and $f_{M_i}|_{M_i}: F_{M_i} \to \mathbb{R}$ be the piecewise linear functions specified in Steps 3 and 4, respectively. Given the barycentric interpolation, we have

$$\mathcal{E}(f_{M_{i-1}}|_{M_{i-1}}) = \mathcal{E}(f_{M'_i}|_{M'_i}), \quad i = m+1, m+2, \dots, n \quad (15)$$

---

[3] Our method does not depend on a specified ordering and any sorting is fine.
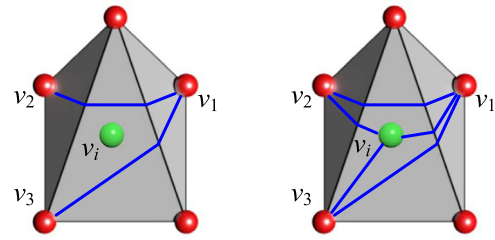
Fig. 3. Insert a vertex v_i into the M_{i-1} (left) and locally split the geodesic triangle $\triangle \widetilde{v_1 v_2 v_3} \in M_{i-1}$ that contains v_i (right).

To see the above property, without loss of generality, we assume that the new added vertex v_i lies inside the geodesic triangle $\triangle \widetilde{v_1 v_2 v_3} \in M_{i-1}$ (Fig. 3 left). By assigning the value $f(v_i)$ using the barycentric interpolation among $f(v_1), f(v_2)$ and $f(v_3)$, and locally subdividing $\triangle \widetilde{v_1 v_2 v_3}$ into three small geodesic triangles $\triangle \widetilde{v_1 v_2 v_i}$, $\triangle \widetilde{v_1 v_i v_3}$ and $\triangle \widetilde{v_i v_2 v_3}$ (Fig. 3 right), it is readily seen that

$$\mathcal{E}(\triangle \widetilde{v_1 v_2 v_3}) = \mathcal{E}(\triangle \widetilde{v_1 v_2 v_i}) + \mathcal{E}(\triangle \widetilde{v_1 v_i v_3}) + \mathcal{E}(\triangle \widetilde{v_i v_2 v_3}) \quad (16)$$

and then Eq. (15) holds. By generalized Rippa's Theorem 1 in [4], the Dirichlet Energy of IDT M_i is not larger than that of M'_i, i.e., $\mathcal{E}(f_{M'_i}|_{M'_i}) \geq \mathcal{E}(f_{M_i}|_{M_i})$. Therefore, we have

$$\mathcal{E}(f|_{I_M}) \geq \mathcal{E}(f_{M'_{m+1}}|_{M'_{m+1}}) \geq \mathcal{E}(f_{M_{m+1}}|_{M_{m+1}}) \geq \mathcal{E}(f_{M'_{m+2}}|_{M'_{m+2}}) \geq \mathcal{E}(f_{M_{m+2}}|_{M_{m+2}}) \geq \cdots \geq \mathcal{E}(f_{M_{n-1}}|_{M_{n-1}}) \geq \mathcal{E}(f_{M'_n}|_{M'_n}) \geq \mathcal{E}(f_{M_n}|_{M_n}) \quad (17)$$

implying $\mathcal{E}(f|_{I_M}) \geq \mathcal{E}(f_{M_n}|_{M_n})$.

Given $V_{M_n} = V_D$ and the assumption of general position in V_D, the intrinsic Delaunay tessellation/triangulation of V_D on D_M is unique [4] and then we have $D_M = M_n$. This indicates that the Dirichlet Energy of IDT I_M is not less than that of D_M by iteratively barycentric interpolation, i.e., $\mathcal{E}(f|_{I_M}) \geq \mathcal{E}(f_{D_M}|_{D_M})$.

By Theorem 3.1, in all possible scalar function $f_D : V_D \to \mathbb{R}$ (including $f_{D_M} = f_{M_n}$ determined by the above iteratively barycentric interpolation and edge flipping process), the function f_D^* specified by holistic COT harmonic interpolation in Proposition 3.1 attains the global minimum of Dirichlet energy. We have

Corollary 3.1. *Given a 2-manifold mesh M, a Delaunay mesh D_M of M and a scalar function $f : V \to \mathbb{R}$, the Dirichlet energy of the function f_D^* specified by Proposition 3.1 on D_M is not larger than the Dirichlet energy of $f|_{I_M}$ on I_M, i.e.,*

$$\mathcal{E}(f_D^*|_{D_M}) \leq \mathcal{E}(f|_{I_M}) \quad (18)$$

Example 3.4. Let $f(v_1) = 1, f(v_2) = 2, f(v_3) = 2$ and $f(v_4) = 2$, the same as in Example 3.1. The DM D_M of the original tetrahedron mesh M in Fig. 2 includes two new vertices v_5 and v_6. Using the holistic COT harmonic interpolation in Proposition 3.1, we have

$$\begin{bmatrix} 153.544 & -51.751 \\ -51.751 & 153.544 \end{bmatrix} \begin{bmatrix} f(v_5) \\ f(v_6) \end{bmatrix} = \begin{bmatrix} 103.545 \\ 103.545 \end{bmatrix} \quad (19)$$

and the solution is $f(v_5) = f(v_6) = 1.0173$. Then the Dirichlet energy on D_M is $\mathcal{E}(f|_{D_M}) = 4.598$, which is smaller than $\mathcal{E}(f|_M)$ and $\mathcal{E}(f|_{I_M})$ (they are computed in Example 3.1), where $f|_{D_M}: F_D \to \mathbb{R}$ is the piecewise linear function on the face set F_D of D_M, interpolating the function values $f(v_i), i = 1, 2, \dots, 6$.

(a) Vase: boundaries between different stripes are more straight in holistic COT harmonic interpolation

(b) Baseball: seam lines are fairer (i.e., with smaller curvature variation in holistic COT harmonic interpolation)

(c) Bread: bread grain stripes are better preserved in holistic COT harmonic interpolation

(d) Turtle: the texture pattern on the foot is more regular in holistic COT harmonic interpolation
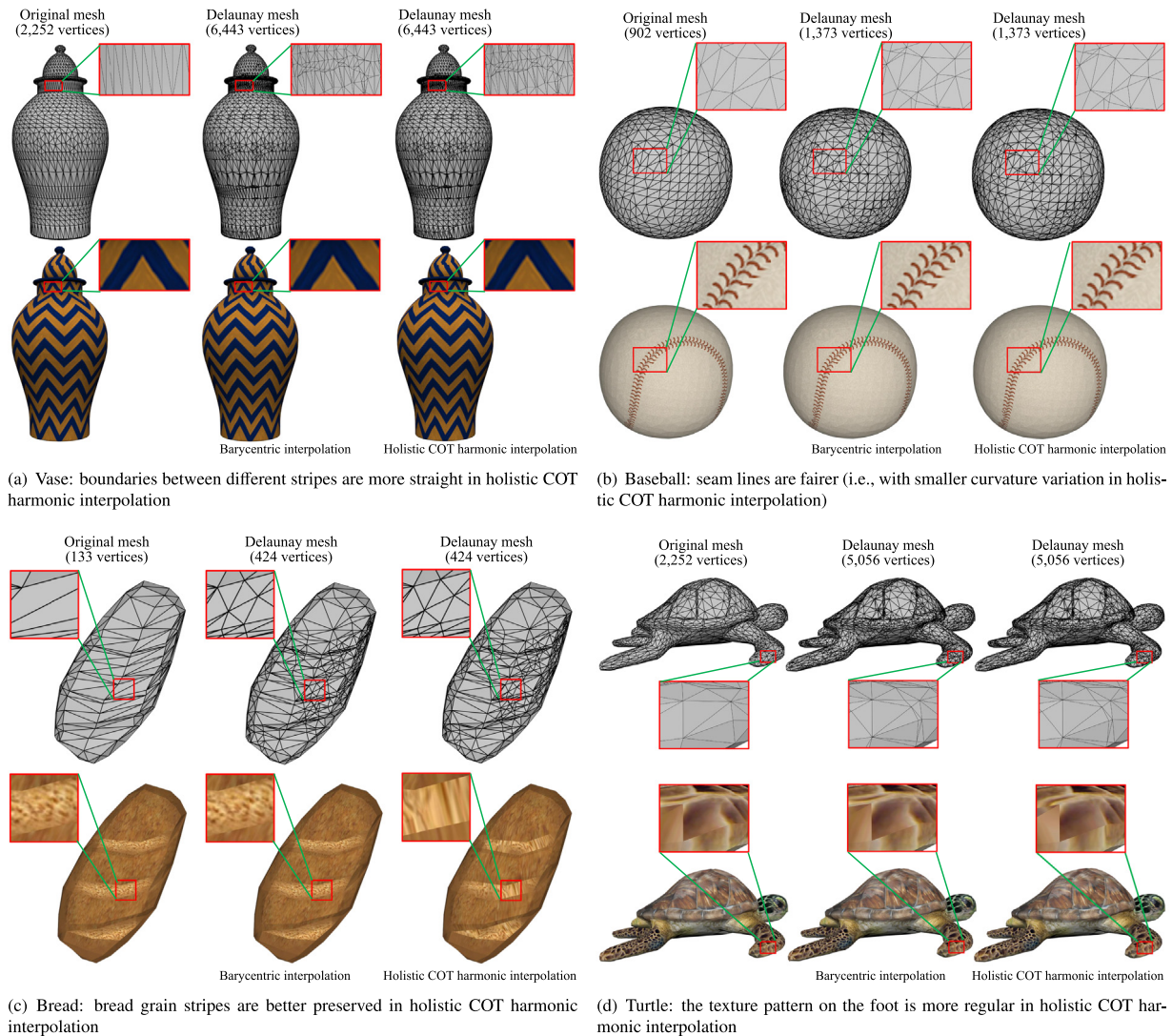
Fig. 4. For many downstream applications, it is desired to convert an arbitrary 2-manifold mesh M into a Delaunay mesh (D_M), which has exactly the same geometry with the original one but is numerically more stable. D_M usually adds more auxiliary vertices into M. To specify the color/texture coordinates at these auxiliary vertices, barycentric interpolation and holistic COT harmonic interpolation can be used. The barycentric interpolation leads to exactly the same color/texture effects on M and D_M (see also Example 3.2). By Theorem 3.1 and Corollary 3.1, holistic COT harmonic interpolation can lead to a minimal Dirichlet Energy on D_M, which is lower than the one by barycentric interpolation, meaning that the color/texture function by holistic COT harmonic interpolation is the smoothest one on D_M.

4. Illustrative examples and discussions

Delaunay meshes are known to have many favorable geometric and numerical behaviors [12] such as more robust geodesic computation using the heat method [15], better accuracy of cotan discrete Laplace–Beltrami operator estimation and better discrete harmonic mapping, etc. Fig. 4 shows some mesh models with colors. For downstream mesh processing such as computing geodesic distances on these models using the heat method, it is suggested to convert the meshes into DMs (which have the same geometry with the original meshes) and perform the computation on DMs [12]. After converting an M into D_M, we need to specify the colors or texture coordinates on those new added vertices $V_D \setminus V$ by interpolating existing colors or texture coordinates on V.

In Fig. 4, two interpolation schemes are used to interpolate texture coordinates. One is the straightforward barycentric interpolation using the original mesh M (which does not change the Dirichlet energy defined on M; see also Example 3.2) and the other is holistic COT harmonic interpolation in Proposition 3.1. Then color images are mapped onto mesh models using texture

coordinates. The results demonstrate that using holistic COT harmonic interpolation leads to much more smooth color/texture distribution on D_M, in accordance with Theorem 3.1 that holistic COT harmonic interpolation achieves the minimization of Dirichlet energy and a lower Dirichlet energy induces a smoother function defined on D_M.

We implemented our algorithm in C++ and evaluated it on eight representative models. Some are commonly used models in graphics community, and others are anisotropic meshes from the Thingi10k dataset.[4] Timings were measured on a workstation (Intel Xeon E5-2620 2 GHz, 32GB RAM). Table 1 reports the run time of IDT and DM construction, barycentric and our interpolation. Although there is no theoretical time complexity, the edge flipping method [4,27] has good practical performance. However, due to the geodesic IDT edges, it is difficult to represent, store and locate geometric primitives in the IDT faces on M. The time efficiency of barycentric interpolation is superior to the proposed interpolation. The main reason is that the time complexity of

---

[4] https://ten-thousand-models.appspot.com/.
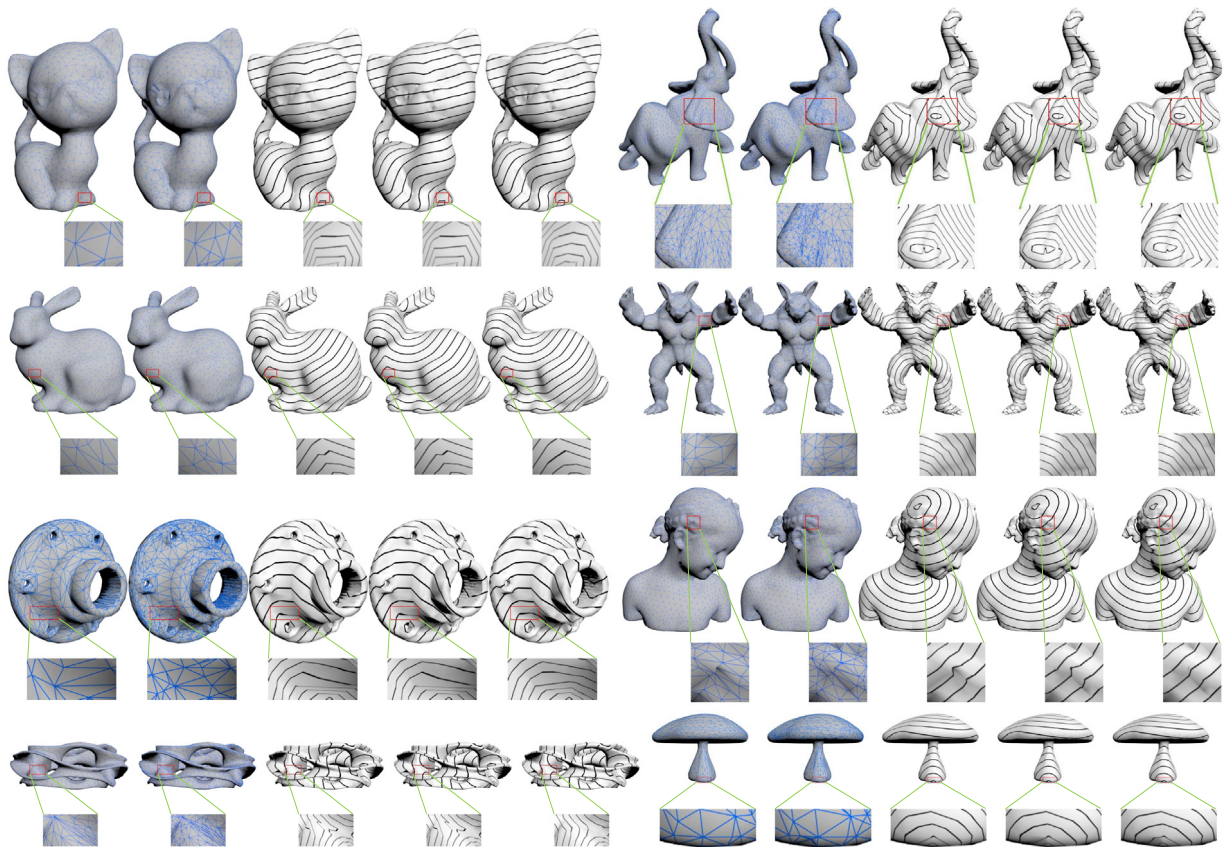
Fig. 5. Interpolating geodesic distances. We compute the exact geodesic distances on the input meshes using the FWP method [29]. Using the geodesic distances on vertices, we adopt barycentric interpolation and our interpolation to compute the distances for the newly added vertices of DM. From left to right, top to bottom: Kitten, Elephant, Bunny, Armadillo, Carter, Bimba, Heptoroid and Mushroom. For each model, the five sub-figures are the input mesh, Delaunay mesh, exact geodesics on the input mesh, barycentric interpolation on DM, and our interpolation on DM. As Table 2 shows, our interpolation has smaller mean and max errors than barycentric interpolation for most models.

Table 1
Quantitative results of running times and Dirichlet Energies (DE) on eight models.

Model name	Input mesh		IDT			DM		Barycentric interpolation		Our interpolation	
	Vert num	DE	Vert num	Time (s)	DE	Vert num	Time (s)	Time (s)	DE	Time (s)	DE
Kitten	1370	0.7933	1370	0.001	0.7773	2146	0.028	0.001	0.7933	0.26	**0.7641**
Bunny	2502	0.5630	2502	0.002	0.5554	3491	0.035	0.001	0.5630	0.413	**0.5469**
Armadillo	3650	1.1076	3650	0.005	1.0852	5884	0.041	0.003	1.1076	0.838	**1.0629**
Elephant	4996	0.7866	4996	0.007	0.7665	9316	0.048	0.005	0.7866	1.581	**0.7459**
Carter	1853	1.6616	1853	0.004	1.5506	6288	0.051	0.028	1.6616	3.315	**1.5449**
Heptoroid	4458	0.6708	4458	0.011	0.6284	17028	0.146	0.016	0.6708	1.808	**0.6164**
Bimba	3099	1.02281	3099	0.004	1.01847	5355	0.04	0.003	1.02881	0.259	**1.01509**
Mushroom	968	3.31713	958	0.002	3.22441	2651	0.022	0.003	3.31713	0.211	**3.2152**

barycentric interpolation is $O(l)$ due to local interpolation, and the time complexity of the proposed interpolation is $O(l^2)$ since the Jacobi iteration is used to solve Eq. (7), where l is the number of unknowns.

Dirichlet energies of the eight models and their DMs are also computed. Our interpolation method achieves the minimal Dirichlet energies on these models (see Table 1). The experimental results also verify our mathematical conclusions. Note that Dirichlet energies are computed based on the geodesic distances.

The iterative interpolation scheme using barycentric coordinates in Section 3.2 (or replacing barycentric interpolation by cotan interpolation in the same iterative scheme) can also result in the Dirichlet energy on D_M no greater than that of IDT I_M. However, both schemes need to construct the IDT of M, and are not globally optimal interpolation with respect to Dirichlet energy. Instead, the proposed interpolation scheme is performed on the original meshes, and achieves global minimization of Dirichlet energies.

In Fig. 5, we estimate the accuracies between our holistic COT harmonic interpolation and the barycentric interpolation on DMs of the eight models. The exact geodesic distances on the input meshes are computed using the FWP method [29]. The geodesic distances of newly added vertices in DMs are estimated by barycentric interpolation and our proposed method, respectively. The relative mean interpolation errors and relative maximal interpolation errors are shown in Table 2. The geodesic contours are visualized in Fig. 5 as well. The experimental results illustrate that the relative mean errors of the proposed method are better than those of the barycentric interpolation in most cases. On the other hand, the relative maximal errors of the proposed interpolation are totally better than those of barycentric interpolation, and moreover the differences are fairly obvious. In extreme cases, the accuracy of barycentric interpolation is

Table 2
Statistics on geodesic interpolation.

Model name	Barycentric interpolation		Our interpolation	
	Mean error (%)	Max error (%)	Mean error (%)	Max error (%)
Kitten	0.4183	237.93	**0.304**	**71.65**
Bunny	0.06	34.59	**0.05**	**16.79**
Armadillo	**0.102**	44.12	0.106	**19.43**
Elephant	0.06	16.72	**0.04**	**16.52**
Carter	0.44	201.34	**0.35**	**36.02**
Heptoroid	0.30	145.82	**0.29**	**23.44**
Bimba	0.23	50.44	**0.09**	**29.30**
Mushroom	0.33	61.72	**0.25**	**25.31**

very bad (e.g., the relative maximal error of Kitten model in Table 2). Therefore the proposed interpolation can well approximate geodesic distances. Particularly, when the geodesic distance field of an input mesh is computed, then the geodesic distance field of *DM* can be directly updated using our proposed interpolation instead of recomputing. Furthermore a geodesic distance γ of an arbitrary point to the source can be estimated using intrinsic barycentric interpolation in *DM*. [5]

5. Conclusion

In this paper, we reveal the relation of Dirichlet energies on DMs and IDT, both of which have the same geometry of the original mesh M. We prove that using a holistic COT harmonic interpolation, we can directly obtain a scalar function $f_D^* : V_D \to \mathbb{R}$ from a given $f : V \to \mathbb{R}$, which achieves the global minimum of Dirichlet energies in all possible functions $f_D : V_D \to \mathbb{R}$ on a given Delaunay mesh D_M. The obtained Dirichlet energy on D_M is no greater than that on IDT I_M. We demonstrate the efficacy of our method on texture mapping and geodesic distance interpolation.

Declaration of competing interest

The authors declare that they have no known competing financial interests or personal relationships that could have appeared to influence the work reported in this paper.

References

[1] Osting B, White CD, Oudet É. Minimal Dirichlet energy partitions for graphs. SIAM J Sci Comput 2014;36(4):1635–51.

[2] Rippa S. Minimal roughness property of the Delaunay triangulation. Comput Aided Geom Design 1990;489–97.

[3] Desbrun M, Meyer M, Alliez P. Intrinsic parameterizations of surface meshes. Comput Graph Forum (Eurographics, 2002) 2002;21(3):209–18.

[4] Bobenko AI, Springborn BA. A discrete Laplace-Beltrami operator for simplicial surfaces. Discrete Comput Geom 2007;38:740–56.

[5] Cheng S-W, Dey TK, Shewchuk J. Delaunay mesh generation. CRC Press; 2012.

[6] Okabe A, Boots B, Sugihara K, Chiu SN. Spatial tessellations: Concept and applications of Voronoi diagrams. Wiley; 2000.

[7] Goes Fd, Memari P, Mullen P, Desbrun M. Weighted triangulations for geometry processing. ACM Trans Graph 2014;33(3):28:1–28:13.

[8] Gong W-Y, Liu Y-J, Tang K, Wu T-R. Approximate Delaunay mesh reconstruction and quality estimation from point samples. J Comput Appl Math 2015;24:23–34.

[9] Rivin I. Euclidean structures on simplicial surfaces and hyperbolic volume. Ann of Math 1994;139(3):553–80.

[10] Pinkall U, Polthier K. Computing discrete minimal surfaces and their conjugates. Experiment Math 1993;2(1):15–36.

[11] Dyer R, Zhang H, Moller T. Delaunay mesh construction. In: Proceedings of the fifth eurographics symposium on geometry processing; 2007. p. 273–82.

[12] Liu Y-J, Xu C-X, Fan D, He Y. Efficient construction and simplification of Delaunay meshes. ACM Trans Graph (ACM SIGGRAPH ASIA 2015) 2015;34(6):174:1–174:13.

[13] Yi R, Liu Y-J, He Y. Delaunay mesh simplification with differential evolution. ACM Trans Graph (ACM SIGGRAPH ASIA 2018) 2018;37(6):263:1–263:12.

[14] Gong W, Yi R, Liu Y-J, He Y. Constructing delaunay mesh with lower energy than intrinsic delaunay triangulation. Commun Inf Syst 2019;3 (2019).

[15] Crane K, Weischedel C, Wardetzky M. Geodesics in heat: A new approach to computing distance based on heat flow. ACM Trans Graph 2013;32(5):152:1–152:11.

[16] Liu Y-J, Fan D, Xu C-X, He Y. Constructing intrinsic Delaunay triangulations from the dual of geodesic Voronoi diagrams. ACM Trans Graph 2017;36(2):15:1–15:15.

[17] Shi-Qing X, Ying X, He Y. Constant-time all-pairs geodesic distance query on triangle meshes. In: Proceedings of the ACM SIGGRAPH symposium on interactive 3D graphics and games; 2012. p. 31–8.

[18] Dziuk G. Finite elements for the Beltrami operator on arbitrary surfaces. In: Partial differential equations and calculus of variations. 1988, p. 142–55.

[19] Frank M. Real analysis and applications : including Fourier series and the calculus of variations. American Mathematical Society; 2005.

[20] Desbrun M, Meyer M, Schröder P, Barr AH. Implicit fairing of irregular meshes using diffusion and curvature flow. In: ACM SIGGRAPH; 1999. p. 317–24.

[21] Meyer M, Desbrun M, Schröder P, Barr AH. Discrete differential-geometry operators for triangulated 2-manifolds. In: Visualization and mathematics III; 2003. p. 35–57.

[22] Wardetzky M, Mathur S, Kälberer F, Grinspun E. Discrete Laplace operators: no free lunch. In: Proceedings of the fifth eurographics symposium on geometry processing; 2007. p. 33–7.

[23] Alexa M, Wardetzky M. Discrete Laplacians on general polygonal meshes. ACM Trans Graph 2011;30(4):102.

[24] Patané G. STAR-Laplacian Spectral kernels and distances for geometry processing and shape analysis. Comput Graph Forum 2016;35(2):599–624.

[25] Xu G. Convergence of discrete Laplace-Beltrami operators over surfaces. Comput Math Appl 2004;48(3–4):347–60.

[26] Xu G, Zhang Q. A general framework for surface modeling using geometric partial differential equations. Comput Aided Geom Design 2008;25(3):181–202.

[27] Fisher M, Springborn B, Bobenko AI, Schroder P. An algorithm for the construction of intrinsic Delaunay triangulations with applications to digital geometry processing. In: ACM SIGGRAPH 2006 Courses; 2006. p. 69–74.

[28] Sharp N, Soliman Y, Crane K. Navigating intrinsic triangulations. ACM Trans Graph 2019;38(4):55.

[29] Xu C, Wang TY, Liu Y-J, Liu L, He Y. Fast wavefront propagation (FWP) for computing exact geodesic distances on meshes. IEEE Trans Vis Comput Graph 2015;21(7):822–34.

---

[5] It means interpolation is performed in IDT.